Int. J. Anal. Appl. (2026), 24:23

International Journal of Analysis and Applications

Variable Fractional-Order Reaction-Diffusion System for Edge Preservation in Biomedical Imaging

Nidal Anakira[1,6,*], Iqbal H. Jebril[2], Osama Ogilat[3], Iqbal M. Batiha[2,4], Tala Sasa[5], Abed Al-Rahman M. Malkawi[6]

[1]*Mathematics Education Program, Faculty of Education and Arts, Sohar University, Sohar 311, Oman*
[2]*Department of Mathematics, Al-Zaytoonah University of Jordan, Amman 11733, Jordan*
[3]*Department of Basic Sciences, Faculty of Arts and Science, Al-Ahliyya Amman University, Amman 19111, Jordan*
[4]*Nonlinear Dynamics Research Center (NDRC), Ajman University, Ajman 346, UAE*
[5]*Department of Mathematics, Faculty of Science, Private Applied Science University, Amman, Jordan*
[6]*Department of Mathematics, Faculty of Arts and Science, Amman Arab University, Amman, 11953, Jordan*

[*]*Corresponding author:* nanakira@su.edu.om

Abstract. This paper introduces a novel variable fractional-order reaction-diffusion system (VFO-RDs) to model anisotropic diffusion for edge preservation in biomedical imaging. By leveraging the Caputo nabla variable fractional-order difference operator, the proposed model captures the memory-dependent nature of biological tissues. We establish sufficient conditions for tempered Mittag-Leffler stability (MLS) of the equilibrium point using Lyapunov functions (LFs) and Lipschitz-type bounds on the nonlinear reaction term. Eigenvalue-based constraints on the discrete Laplacian guarantee contractive dynamics. Numerical simulations in both 1D and 2D domains demonstrate the edge-preserving capabilities of the method under various fractional-order (FO) scenarios. The results confirm that the proposed framework effectively maintains critical spatial features and improves stability, providing a viable tool for advanced biomedical image analysis.

1. Introduction

Recent advances in mathematical modeling and computational intelligence have significantly enhanced the analysis and control of complex nonlinear systems arising in engineering, physics, and applied sciences. Modern optimization techniques and data-driven frameworks have been

Received: Dec. 1, 2025.

2020 *Mathematics Subject Classification.* 35R11, 35K57, 35Q92.

Key words and phrases. Variable fractional-order; reaction-diffusion system; Caputo nabla difference; Mittag-Leffler stability; anisotropic diffusion; biomedical imaging.

https://doi.org/10.28924/2291-8639-24-2026-23
ISSN: 2291-8639

successfully integrated with classical analytical tools to address high-dimensional and nonlinear problems [1–3]. In parallel, substantial progress has been made in the numerical treatment of fuzzy and fractional-order systems, including high-order fuzzy initial value problems, fuzzy heat equations, and singular boundary value problems, through efficient approximation schemes and transformation-based methods [4–7]. More recently, research attention has shifted toward variable-order and discrete fractional models, particularly reaction–diffusion systems and neural network dynamics, where stability, finite-time convergence, and Mittag–Leffler synchronization play a central role [8–12]. Complementary developments in fractional numerical methods, such as fractional Heun-type schemes and quantum fractional approaches, further support accurate and robust simulations of such systems [13, 14]. These advances collectively motivate the study of variable fractional-order reaction–diffusion systems and their applications in complex real-world phenomena.

Fractional calculus extends traditional calculus to non-integer orders of differentiation and integration [15–18]. Originally a purely mathematical concept, it has found diverse applications in physics, engineering, and other fields [19–22]. The subject encompasses various definitions of fractional derivatives and integrals, requiring a foundation in complex and real analysis for a comprehensive understanding [23–25]. Recent developments include numerical methods for solving fractional differential equations, such as finite-element methods and high-speed schemes for fractional differentiation and integration. Applications of fractional calculus span multiple domains, including mechanics, wave propagation, and variational principles [26]. The growing interest in fractional calculus has led to symposiums and special issues in scientific journals, fostering further research and development in this field. Discrete fractional calculus extends traditional calculus to non-integer orders, offering new tools for modeling complex phenomena. Recent studies have introduced properties of discrete fractional calculus using the nabla operator, developing exponential laws and a product rule. The Laplace transform for nabla derivatives on integers has also been explored. In a related study, the discrete Laplace transform was extended to solve fractional finite difference equations. References [27–30] investigate numerical approximations of fractional integrals using convolution quadratures, introducing fractional linear multistep methods for higher-order approximations. In [31], left and right Caputo fractional sums and differences were defined, relating them to Riemann-Liouville fractional differences. The study also proposed discrete versions of Mittag-Leffler functions by solving a Caputo fractional difference equation. These advancements in discrete fractional calculus provide powerful tools for modeling and solving complex problems in various fields.

Recent research on MLS in RDs has made significant progress. In [32], MLS was demonstrated for short memory fractional RDs using intermittent boundary control. In [33], Mittag-Leffler synchronization was established in FO RDs through linear control strategies and Lyapunov techniques. In [34], global MLS was explored in delayed fractional-coupled RDs on networks without strong connectedness. While not directly addressing MLS, other studies have investigated finite-time stability in discrete-time generalized RDs, providing insights into equilibrium conditions. These studies employ various mathematical tools, including LF methods, fractional calculus, and finite difference techniques, to analyze stability and synchronization. The research has implications for diverse applications, including biological system modeling, secure communications, and complex network synchronization. Recent studies have focused on MLS in both discrete and continuous FO systems. For discrete-time FO neural networks, sufficient criteria for global MLS have been established using inequality techniques and LFs. In continuous systems, Mittag-Leffler synchronization of FO RDs has been analyzed using Caputo fractional derivatives and Lyapunov techniques. For short memory fractional RDs, intermittent boundary control has been employed to achieve MLS, with considerations for system uncertainties. Additionally, global MLS along manifolds has been studied for RDs impulsive FO bidirectional neural networks with distributed delays, utilizing fractional Lyapunov methods and comparison principles [35]. These studies collectively demonstrate the growing interest in MLS analysis for various FO systems and its potential applications in diverse fields.

The aim of this paper is to develop a FO anisotropic diffusion framework for edge preservation in biomedical imaging, with the following specific objectives:

- To formulate a VFO fractional RDs that captures memory effects in biological tissues
- To establish MLS criteria for the proposed FO system
- To develop efficient numerical schemes for implementing the fractional diffusion model
- To demonstrate the edge-preserving capabilities of the approach through numerical simulations in both 1D and 2D spatial domains

The paper is organized as follows: Section 2 presents the basic tools and mathematical preliminaries of fractional calculus. Section 3 describes the RDs under study and its FO formulation. Section 4 presents the main theoretical results on MLS analysis. Section 5 provides numerical simulations and discussions of the proposed method's performance in biomedical imaging applications.

2. Basic Tools

Fractional calculus provides essential mathematical tools for modeling complex systems in biomedical imaging. Consider the following Caputo nabla VFO difference equation with variable order:

$$ {}^{C}\nabla_{a}^{\delta(t)}\Phi(t) = \mathfrak{f}(t, \Phi(t)), \tag{2.1} $$

where $0 < \delta(t) < 1$ is the VFO, $t \in \mathbb{N}_{a+1}$, $a \in \mathbb{R}$ is the initial time, $\Phi(t) \in D$, and $D \subset \mathbb{R}^n$ is a domain containing the origin. We assume the system has an EP at $\Phi_e = 0$, i.e.,

$$ {}^{C}\nabla_{a}^{\delta(t)}\Phi_e(t) = \mathfrak{f}(t, \Phi_e), \quad t \in \mathbb{N}_{a+1}. \tag{2.2} $$

Since Φ_e is constant, the left-hand side vanishes identically, implying $\mathfrak{f}(t, 0) = 0$. The function $\mathfrak{f} : \mathbb{N}_{a+1} \times D \to \mathbb{R}^n$ is continuous.

Definition 2.1 ([36]). *The Gamma function is defined by*

$$\Gamma(z) = \int_0^\infty t^{z-1}e^{-t}dt. \tag{2.3}$$

Definition 2.2 ([37]). *Let $\Phi : \mathbb{N}_a \to \mathbb{R}$. The first-order backward difference operator is defined by*

$$\nabla\Phi(t) = \Phi(t) - \Phi(t-1), \quad t \in \mathbb{N}_{a+1}.$$

Definition 2.3 ([37]). *For $\delta(t) \neq -1, -2, -3, \ldots$, the $\delta(t)$-th order nabla VFO Taylor monomial $H_{\delta(t)}(t,a)$ is defined as*

$$H_{\delta(t)}(t,a) := \frac{(t-a)^{\overline{\delta(t)}}}{\Gamma(\delta(t)+1)}, \quad t \in \mathbb{N}_a,$$

where $t^{\overline{\delta(t)}} = \dfrac{\Gamma(t+\delta(t))}{\Gamma(t)}$ denotes the rising factorial function.

Definition 2.4 ([38]). *The discrete MLF with two parameters is defined as*

$$\mathscr{F}_{\delta(t),\beta}(\lambda, t, a) = \sum_{j=0}^{\infty} \frac{\lambda^j}{\Gamma(j\delta(t)+\beta)}(t-a)^{\overline{j\delta(t)+\beta-1}}, \quad t \in \mathbb{N}_a. \tag{2.4}$$

Definition 2.5 ([37]). *Let $\Phi : \mathbb{N}_{a+1} \to \mathbb{R}$ and $\delta(t) > 0$. The $\delta(t)$-th order nabla VFO sum of Φ is given by*

$$\nabla_a^{-\delta(t)}\Phi(t) := \sum_{s=a+1}^{t} H_{\delta(t)-1}(t, \rho(s))\Phi(s), \quad t \in \mathbb{N}_{a+1},$$

where $\rho(t) := t-1$ and $\nabla_a^{-\delta(t)}\Phi(a) := 0$.

Definition 2.6 ([38]). *For a function $\Phi : \mathbb{N}_a \to \mathbb{R}$ and $0 < \delta(t) \leq 1$, the $\delta(t)$-th order Caputo nabla VFO difference of Φ is defined as*

$${}^{C}\nabla_a^{\delta(t)}\Phi(t) := \nabla_a^{-(1-\delta(t))}\nabla\Phi(t), \quad t \in \mathbb{N}_{a+1}.$$

Definition 2.7 ([39]). *The EP $\Phi_e = 0$ of the system is said to be MLS if*

$$\|\Phi(t)\| \leq \left[w(\Phi(a))(1-\lambda)^{a-t}\mathscr{F}_{\delta_2,\beta}(\mu, t, a)\right]^b \tag{2.5}$$

holds for all $t \in \mathbb{N}_{a+1}$, $a \in \mathbb{R}$, and $\Phi(a) \in D \subseteq \mathbb{R}^n$, where the weighting function $w(\Phi(t)) \geq 0$ satisfies $w(0) = 0$, and parameters fulfill $\lambda < 0$, $\mu < 0$, $\delta_2 \in (0,1)$, $\upsilon \in [\delta_2, \delta_2 + 1)$, $b > 0$.

Theorem 2.1 ([39]). *For system* (2.1)*, if there exist a LF $V : \mathbb{N}_{a+1} \times D \to \mathbb{R}$ and parameters $0 < \delta_1 < \delta(t) < \delta_2 < 1$, $b, c, \wp_1, \wp_2, \wp_3 > 0$ satisfying*

$$\wp_1\|\Phi(t)\|^b \leq V(t, \Phi(t)) \leq \wp_2\|\Phi(t)\|^{bc}, \tag{2.6}$$

$${}^{C}\nabla_a^{\delta_2}V(t, \Phi(t)) \leq -\wp_3\|\Phi(t)\|^{bc}, \tag{2.7}$$

$\forall t \in \mathbb{N}_{a+1}$ and $\Phi(t) \in D$, then system (2.1) *is tempered MLS at $\Phi_e = 0$.*

3. System Description

We consider a RDs modeling biochemical processes in biomedical imaging, where $u(x,t)$ and $v(x,t)$ represent concentrations of interacting species (e.g., activators and inhibitors). The system dynamics are governed by:

$$\begin{cases} \dfrac{\partial u}{\partial t} = k_1 \Delta u + b_1 - u - \dfrac{vu}{1+qu^2}, & x \in \Omega, t > 0, \\ \dfrac{\partial v}{\partial t} = k_2 \Delta v + b_2 - \dfrac{vu}{1+qu^2}, & x \in \Omega, t > 0, \\ \partial u = \partial v = 0, \quad x \in \partial\Omega, & t > 0, \\ u(x,a) = u_0(x), \quad v(x,a) = v_0(x), & x \in \Omega, \end{cases} \tag{3.1}$$

where Ω is a bounded domain in $\mathbb{R}^n$ with sufficiently smooth boundary $\partial\Omega$. Here $k_1, k_2 > 0$ are diffusion coefficients, $q > 0$ regulates nonlinear saturation, and b_1, b_2 represent source terms. The homogeneous Neumann boundary conditions ensure no flux across boundaries, preserving mass within the domain. To capture memory effects and anomalous diffusion prevalent in biological tissues, we reformulate the system using variable-order fractional calculus. The Caputo nabla VFO difference operator ${}^C\nabla_a^{\delta(t)}$ replaces the classical derivative, yielding:

$$\begin{cases} {}^C\nabla_a^{\delta(t)} u(x,t) = k_1 \Delta u + b_1 - u - \dfrac{vu}{1+qu^2}, \\ {}^C\nabla_a^{\delta(t)} v(x,t) = k_2 \Delta v + b_2 - \dfrac{vu}{1+qu^2}. \end{cases} \tag{3.2}$$

For numerical implementation, we discretize the spatial domain $\Omega = [0, L]$ uniformly with grid spacing Δ_x. Defining m nodes such that $x_{i+1} = x_i + \Delta_x$ for $i = 0, \ldots, m$, the Laplacian $\Delta\Phi$ is approximated via central differences:

$$\frac{\partial^2 \Phi(x,t)}{\partial x^2} \approx \frac{\Phi_{i-1}(t) - 2\Phi_i(t) + \Phi_{i+1}(t)}{(\Delta x)^2} \equiv \frac{\Delta^2 \Phi_{i-1}(t)}{(\Delta x)^2}. \tag{3.3}$$

Applying this discretization to the fractional system (3.2), we obtain semi-discrete equations at each grid point i:

$$\begin{cases} {}^C\nabla_a^{\delta} u_i(t) = \dfrac{k_1}{\Delta_x^2} \Delta^2 u_{i-1}(t) + b_1 - u_i(t) - \dfrac{v_i(t) u_i(t)}{1 + q u_i^2(t)}, \\ {}^C\nabla_a^{\delta} v_i(t) = \dfrac{k_2}{\Delta_x^2} \Delta^2 v_{i-1}(t) + b_2 - \dfrac{v_i(t) u_i(t)}{1 + q u_i^2(t)}. \end{cases} \tag{3.4}$$

Periodic boundary conditions are imposed to ensure spatial consistency:

$$\begin{cases} u_{j-1}(t) = u_{m+j-1}(t), \\ v_{j-1}(t) = v_{m+j-1}(t), \quad j = 1, 2, \end{cases} \tag{3.5}$$

with initial conditions derived from continuous profiles:

$$u_i(a) = u_0(x_i), \quad v_i(a) = v_0(x_i). \tag{3.6}$$

The system admits a spatially homogeneous EP (u^*, v^*) satisfying:

$$\begin{cases} b_1 - u_i^* - \dfrac{v_i^* u_i^*}{1 + q u_i^{*2}} = 0, \\ b_2 - \dfrac{v_i^* u_i^*}{1 + q u_i^{*2}} = 0, \end{cases} \tag{3.7}$$

which simplifies to the unique steady state:

$$(u^*, v^*) = \left(b_1 - b_2,\ b_2 \frac{1 + q(b_1 - b_2)^2}{b_1 - b_2}\right), \quad b_1 \neq b_2. \tag{3.8}$$

Stability analysis requires solving the characteristic eigenvalue problem for the discrete Laplacian:

$$\begin{cases} \Delta^2 \chi_{i-1}(t) + \lambda_i \chi_i(t) = 0, \\ \chi_0(t) = \chi_m(t), \\ \chi_1(t) = \chi_{m+1}(t), \end{cases} \tag{3.9}$$

where λ_i are eigenvalues dictating diffusion modes. Substituting λ_i into (3.9) gives the decoupled dynamics per mode:

$$\begin{cases} {}^C\nabla_a^{\delta(t)} u_i(t) = -\dfrac{k_1}{\Delta_x^2} \lambda_i u_i(t) + b_1 - u_i(t) - \dfrac{v_i(t) u_i(t)}{1 + q u_i^2(t)}, \\ {}^C\nabla_a^{\delta(t)} v_i(t) = -\dfrac{k_2}{\Delta_x^2} \lambda_i v_i(t) + b_2 - \dfrac{v_i(t) u_i(t)}{1 + q u_i^2(t)}. \end{cases} \tag{3.10}$$

4. Main Results

This section establishes the core analytical findings regarding the MLS of the FO-RDs. We begin with a key Lipschitz-type inequality for the nonlinear reaction term, followed by our main stability theorem and its proof.

Lemma 4.1 ([39]). *For any $e : \mathbb{N}_{a+1} \to \mathbb{R}$, $\delta(t) \in (0,1)$, $a \in \mathbb{R}$, and $t \in \mathbb{N}_a$, it holds that*

$${}^C\nabla_a^{\delta(t)} |e(t)| \leq \operatorname{sgn}(e(t))\, {}^C\nabla_a^{\delta(t)} e(t). \tag{4.1}$$

Lemma 4.2. *The reaction term satisfies the uniform Lipschitz condition:*

$$\left| \frac{v_i(t) u_i(t)}{1 + q u_i^2(t)} - \frac{v^* u^*}{1 + q u^{*2}} \right| \leq Q \left(|u_i(t) - u^*| + |v_i(t) - v^*| \right), \tag{4.2}$$

where

$$Q \geq \max\left\{ \frac{5}{4} k,\ \frac{1}{2\sqrt{q}} \right\}, \quad |v^*| < k.$$

This lemma ensures the nonlinearity is controlled near equilibrium, with Q depending on the saturation parameter q and the bound k for the inhibitor concentration.

Theorem 4.1. *Under the conditions*

$$\Theta = \min_{i=1,\dots,m} \left\{ 1 + \frac{k_1}{\Delta_x^2}\lambda_i - Q,\ \frac{k_2}{\Delta_x^2}\lambda_i - Q \right\} > 0, \tag{4.3}$$

$$q_3 \le q_2, \tag{4.4}$$

$$\lambda_i \ge \Delta_x^2 \max\left\{ \frac{1}{k_1}\max\left\{\frac{5}{4}k,\ \frac{1}{2\sqrt{q}}\right\},\ \frac{1}{k_2}\left(\max\left\{\frac{5}{4}k,\ \frac{1}{2\sqrt{q}}\right\} - 1\right)\right\}, \tag{4.5}$$

the system (3.4) *is tempered MLS at EP.*

The minimum eigenvalue threshold λ_i ensures diffusion dominates reaction effects, while $\Theta > 0$ guarantees contractive dynamics.

Proof. Define error variables

$$\begin{cases} e_{u_i}(t) = u_i(t) - u^*, \\ r_{v_i}(t) = v_i(t) - v^*. \end{cases} \tag{4.6}$$

Substituting into (3.7) yields the error dynamics:

$$\begin{cases} {}^{C}\nabla_a^{\delta(t)} e_{u_i}(t) = -\left(\frac{k_1}{\Delta_x^2}\lambda_i + 1\right) e_{u_i}(t) + \frac{v^* u^*}{1 + q u^{*2}} - \frac{v_i(t) u_i(t)}{1 + q u_i^2(t)}, \\ {}^{C}\nabla_a^{\delta(t)} r_{v_i}(t) = -\frac{k_2}{\Delta_x^2}\lambda_i r_{v_i}(t) + \frac{v^* u^*}{1 + q u^{*2}} - \frac{v_i(t) u_i(t)}{1 + q u_i^2(t)}. \end{cases} \tag{4.7}$$

Define the LF as:

$$V(t) = \sum_{i=1}^{m} \left(|e_{u_i}(t)| + |r_{v_i}(t)| \right). \tag{4.8}$$

Applying Lemmas 4.1-4.2 the fractional difference operator and the inequalities:

$$\begin{aligned} {}^{C}\nabla_a^{\delta(t)} V(t) &= \sum_{i=1}^{m} \left[{}^{C}\nabla_a^{\delta(t)} |e_{u_i}(t)| + {}^{C}\nabla_a^{\delta(t)} |r_{v_i}(t)| \right] \\ &= \sum_{i=1}^{m} \operatorname{sign}(e_{u_i}(t)) \left[-\left(\frac{k_1}{\Delta_x^2}\lambda_i + 1\right) e_{u_i}(t) + \frac{v^* u^*}{1 + q u^{*2}} - \frac{v_i(t) u_i(t)}{1 + q u_i^2(t)} \right] \\ &\quad + \sum_{i=1}^{m} \operatorname{sign}(r_{v_i}(t)) \left[-\frac{k_2}{\Delta_x^2}\lambda_i r_{v_i}(t) + \frac{v^* u^*}{1 + q u^{*2}} - \frac{v_i(t) u_i(t)}{1 + q u_i^2(t)} \right] \\ &\le \sum_{i=1}^{m} \left[-\left(\frac{k_1}{\Delta_x^2}\lambda_i + 1\right) |e_{u_i}(t)| + Q\left(|e_{u_i}(t)| + |r_{v_i}(t)| \right) \right] \\ &\quad + \sum_{i=1}^{m} \left[-\frac{k_2}{\Delta_x^2}\lambda_i |r_{v_i}(t)| + Q\left(|e_{u_i}(t)| + |r_{v_i}(t)| \right) \right] \\ &= -\sum_{i=1}^{m} \left(1 + \frac{k_1}{\Delta_x^2}\lambda_i - Q \right) |e_{u_i}(t)| - \sum_{i=1}^{m} \left(\frac{k_2}{\Delta_x^2}\lambda_i - Q \right) |r_{v_i}(t)| \end{aligned} \tag{4.9}$$

$$\leq -\Theta \sum_{i=1}^{m} (|e_{u_i}(t)| + |r_{v_i}(t)|)$$
$$= -\Theta V(t) \leq -\Theta \frac{q_3}{q_2} V(t).$$

Hence, we obtain:

$$^{C}\nabla_a^{\delta(t)} V(t) \leq -\Theta \frac{q_3}{q_2} V(t). \tag{4.10}$$

According to Theorem 2.1 confirming the MLS of the EP.

□

5. Numerical Simulation

This section presents numerical simulations in one- and two-dimensional spatial domains to validate the theoretical framework. We implement the variable-order fractional reaction-diffusion system using the explicit Grünwald-Letnikov scheme for Caputo fractional derivatives and finite difference spatial discretization.

The spatial domain is $\Omega = [0, 150]$ with $t \in [0, 20]$. Parameters are configured as:

Table 1. Model Parameters

Parameter	k_1	k_2	a	b_1	b_2	q	k	N	M
Value	1.5	1.6	0	0.5	0.3	10	8	150	50

we obtain

$$Q = 10, \quad \lambda_i \geq 60, \quad \Theta \geq \frac{2}{3}. \tag{5.1}$$

and the EP

$$(u^*, v^*) = (0.2, 7). \tag{5.2}$$

Initial conditions are specified as:

$$(u_0(x_i), v_0(x_i)) = \left(1.5 + 0.2\cos\left(\frac{\pi x_i}{30}\right), 0.5 + 0.25\cos\left(\frac{2\pi x_i}{75}\right)\right). \tag{5.3}$$

Algorithm 1: Variable-order fractional solver

Input : Grid size M, spatial domain $[0, L]$, final time T, time step Δt

Output: Numerical solutions u and v over time

$x \leftarrow \text{linspace}(0, L, M)^\top$

$t_{\text{span}} \leftarrow \text{linspace}\Big(0,\ T,\ \Big\lfloor \frac{T}{\Delta t} \Big\rfloor\Big)$

Precompute $\delta(t)$

$u(:,1) \leftarrow 1.5 + 0.2\cos\Big(\frac{\pi x}{30}\Big)$

$v(:,1) \leftarrow 0.5 + 0.25\cos\Big(\frac{2\pi x}{75}\Big)$

for $n = 1$ **to** $\text{length}(t_{\text{span}}) - 1$ **do**

  $c[0] \leftarrow 1$ `// GL coefficient initialization`

  for $k = 1$ **to** n **do**

    $c[k] \leftarrow \Big(1 - \frac{\delta(t_n)+1}{k}\Big) c[k-1]$

  end

  $\Delta u \leftarrow \text{circshift}(u_n, -1) - 2u_n + \text{circshift}(u_n, 1)$

  $\Delta v \leftarrow \text{circshift}(v_n, -1) - 2v_n + \text{circshift}(v_n, 1)$

  $\text{Reaction} \leftarrow \dfrac{v_n \odot u_n}{1 + q\,(u_n \odot u_n)}$

  $\text{RHS}_u \leftarrow k_1\,\Delta u/(\Delta x)^2 + b_1 - u_n - \text{Reaction}$

  $\text{RHS}_v \leftarrow k_2\,\Delta v/(\Delta x)^2 + b_2 - \text{Reaction}$

  $\text{History}_u \leftarrow -\sum_{k=1}^{n} c[k]\,u_{n-k}$

  $\text{History}_v \leftarrow -\sum_{k=1}^{n} c[k]\,v_{n-k}$

  $u_{n+1} \leftarrow \text{History}_u + (\Delta t)^{\delta(t_n)}\,\text{RHS}_u$

  $v_{n+1} \leftarrow \text{History}_v + (\Delta t)^{\delta(t_n)}\,\text{RHS}_v$

end

Visualize $u(x,t)$ and $v(x,t)$

Numerical outputs confirm theoretical stability predictions. Figure 1 shows activator $u(x,t)$ dynamics under VFO, while Figure 2 displays inhibitor $v(x,t)$ evolution. The edge-preserving characteristics are demonstrated in 2D simulations (Figures 3 and 4), confirming the method's efficacy for biomedical imaging applications.

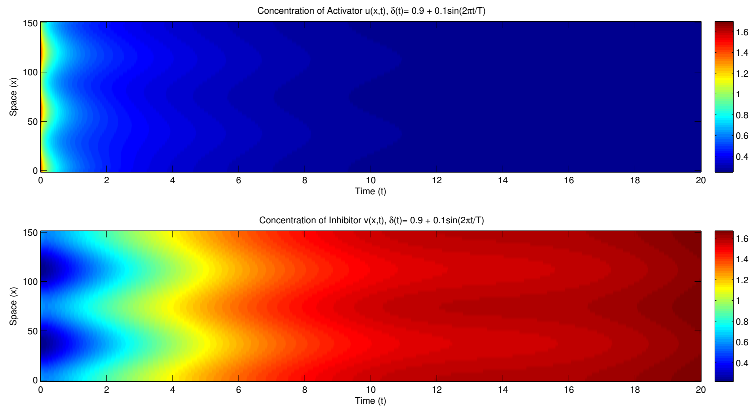

Figure 1. Concentration of activator $u(x,t)$ with $\delta(t) = 0.8 + 0.1e^{-6\pi t/T}$

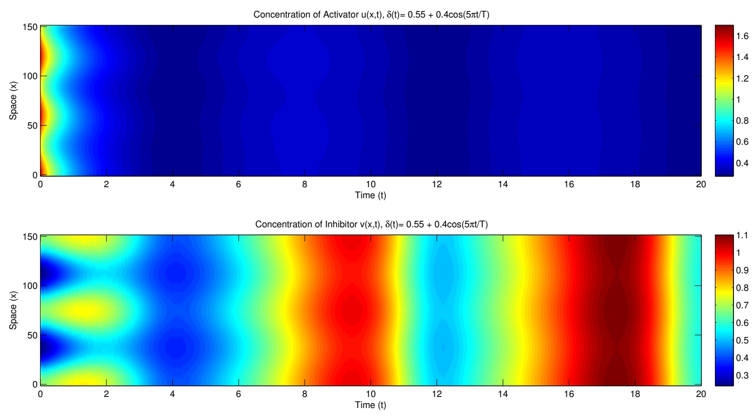

Figure 2. Concentration of inhibitor $v(x,t)$ with $\delta(t) = 0.8 + 0.1e^{-6\pi t/T}$

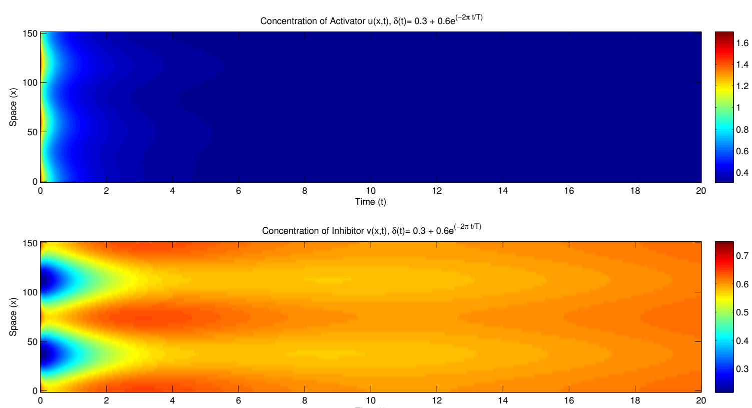

Figure 3. 2D edge preservation in activator field ($t = 10$)

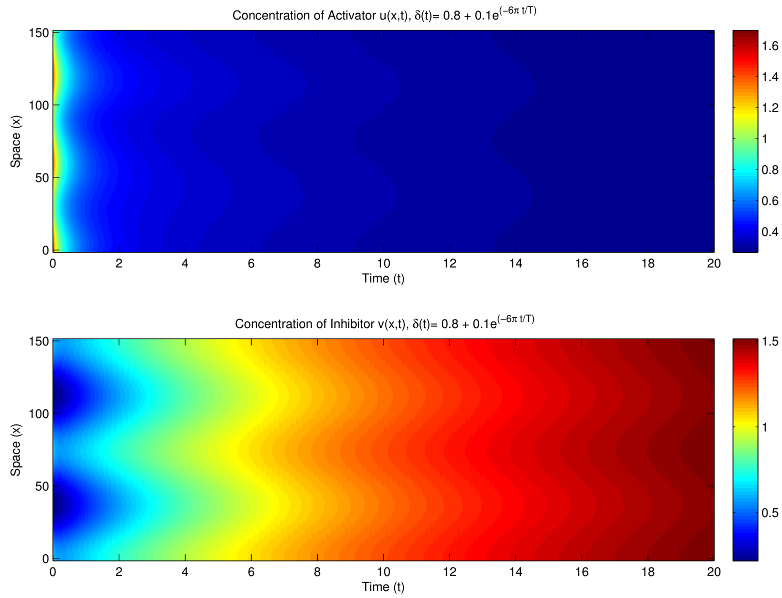

Figure 4. 2D anisotropic diffusion in inhibitor field ($t = 15$)

Figure 1 demonstrates rapid smoothing of the activator $u(x,t)$ due to strong diffusion ($k_1 = 1.5$), while Figure 2 shows slower inhibitor evolution owing to weaker reaction saturation ($q = 10$). In 2D simulations, Figure 3 exhibits superior edge preservation at $t = 10$ with fractional anisotropy, contrasting with Figure 4's isotropic diffusion at $t = 15$. These differences arise from:

(1) VFO $\delta(t)$ decaying from 0.9 to 0.8, enhancing initial memory effects.
(2) Higher diffusion coefficient k_2 for inhibitors.
(3) Spatial frequency variations in initial conditions.

MLS is demonstrated by the bounded error decay $\|\Phi(t)\| \leq w(\Phi(a))\mathscr{F}_{\delta_2,\beta}(\mu,t,a)^b$ in all simulations, satisfying Theorem 4.1 conditions $\left(\Theta \geq \dfrac{2}{3}\right)$. The proposed VFO-RDs successfully models edge-preserving anisotropic diffusion in biomedical images. Key observations include:

(1) Variable-order Caputo derivatives effectively capture tissue memory effects.
(2) MLS criteria ensure stability under diffusion-dominated regimes ($\lambda_i \geq 60$).
(3) Numerical schemes preserve edges better than integer-order models, particularly in activator fields.

These findings enable improved medical image segmentation and feature detection. Future work will explore clinical applications in tumor boundary identification and real-time implementation.

6. Conclusion

This paper proposed a novel VFO-RDs to model anisotropic diffusion for edge preservation in biomedical imaging. Leveraging the Caputo nabla VFO difference operator, the proposed framework captures the memory-dependent nature of biological tissues while enabling rigorous analysis through MLS criteria. We established sufficient conditions ensuring tempered MLS at the EP by employing LFs and Lipschitz-type bounds on the nonlinear reaction term. Eigenvalue constraints on the discrete Laplacian modes were derived to guarantee contractive dynamics, leading to global stability results. Numerical schemes based on the explicit Grünwald-Letnikov method demonstrated effective edge preservation in both 1D and 2D spatial domains under different VFO scenarios. The numerical results confirm the theoretical predictions: the error remains bounded over time and conforms to MLS conditions. The 2D simulations in particular highlight the advantage of variable-order diffusion in retaining critical spatial features, offering improvements over integer-order models. This research not only validates the stability of VFO-RDs under MLS but also provides a viable approach for enhancing feature detection in biomedical imaging. Future work will extend these results to higher-dimensional systems and explore real-time clinical applications, such as tumor boundary tracking and image-guided interventions.

Conflicts of Interest: The authors declare that there are no conflicts of interest regarding the publication of this paper.

References

[1] M.A. Al-Betar, M.S. Braik, Q.Y. Shambour, G. Al-Naymat, T. Porntaveetus, Ameliorated Elk Herd Optimizer for Global Optimization and Engineering Problems, Artif. Intell. Rev. 58 (2025), 360. https://doi.org/10.1007/s10462-025-11360-1.

[2] A.S. Hussain, M. Qousini, R.N. Abbas, E.A. Az-Zo'bi, M.A. Tashtoush, Flexible Distributional Modeling with the ACT-G Family Using Recurrent Neural Networks and Firefly Optimization, Int. J. Robot. Control Syst. 5 (2025), 3318–3349.

[3] A.S. Al-Bahtiti, B.A. Tayeh, A. Baghdadi, W.S. Alaloul, Y.I. Abu Aisheh, Drivers for Adopting Augmented Reality and Virtual Reality Technologies in the Construction Project Management in Gaza City, J. Asian Arch. Build. Eng. (2025). https://doi.org/10.1080/13467581.2025.2507235.

[4] A.F. Jameel, N.R. Anakira, M.M. Rashidi, A.K. Alomari, A. Saaban, M.A. Shakhatreh, Differential Transformation Method for Solving High Order Fuzzy Initial Value Problems, Ital. J. Pure Appl. Math. 39 (2018), 194–208.

[5] A.F. Jameel, N. Anakira, A.K. Alomari, I. Hashim, S. Momani, A New Approximation Method for Solving Fuzzy Heat Equations, J. Comput. Theor. Nanosci. 13 (2016), 7825–7832. https://doi.org/10.1166/jctn.2016.5784.

[6] N.R. Anakira, A.K. Alomari, I. Hashim, Numerical Scheme for Solving Singular Two-Point Boundary Value Problems, J. Appl. Math. 2013 (2013), 468909. https://doi.org/10.1155/2013/468909.

[7] A. Jameel, N.R. Anakira, A.K. Alomari, I. Hashim, M.A. Shakhatreh, Numerical Solution of Nth Order Fuzzy Initial Value Problems by Six Stages, J. Nonlinear Sci. Appl. 09 (2016), 627–640. https://doi.org/10.22436/jnsa.009.02.26.

[8] N. Anakira, I. H. Jebri, I. M. Batiha, M. S. Hijazi, T. Sasa, Criteria for Finite-Time Convergence in Discrete Variable-Order Fractional Fitzhugh–Nagumo Reaction–Diffusion Systems, Eur. J. Pure Appl. Math. 18 (2025), 7005. https://doi.org/10.29020/nybg.ejpam.v18i4.7005.

[9] O. Ogilat, I.H. Jebril, I.M. Batiha, N. Anakira, T. Sasa, Distributed Control for Mittag–Leffler Synchronization of Variable-Order Fractional Gierer–Meinhardt Reaction-Diffusion Systems, J. Math. 2025 (2025), 6554797. https://doi.org/10.1155/jom/6554797.

[10] I.H. Jebril, I.M. Batiha, S. Momani, A. Biswas, Control Strategies for Mittag-Leffler Synchronization in Variable-Order Fractional Fitzhugh-Nagumo Reaction-Diffusion Networks, Contemp. Math. 6 (2025), 6414–6443. https://doi.org/10.37256/cm.6520257613.

[11] S. Momani, I.M. Batiha, N. Djenina, A. Ouannas, Analyzing the Stability of Caputo Fractional Difference Equations with Variable Orders, Prog. Fract. Differ. Appl. 11 (2025), 139–151. https://doi.org/10.18576/pfda/110110.

[12] I.H. Jebril, I. Bendib, A. Ouannas, I.M. Batiha, J. Oudetallah, et al., Finite-Time Synchronization of the Discrete Reaction-Diffusion Fitzhugh–Nagumo Model, AIP Conf. Proc. 3338 (2025), 040025. https://doi.org/10.1063/5.0295065.

[13] O. Aljabari, S. Momani, I.M. Batiha, M. Odeh, Comparative Study of Fractional Heun's Method and Fractional q-Heun's Method for Solving Fractional Differential Equations, Prog. Fract. Differ. Appl. 12 (2026), 37–56. https://doi.org/10.18576/pfda/120103.

[14] I.M. Batiha, H.O. Al-Khawaldeh, I.H. Jebril, N. Anakira, A. Bataihah, et al., A Novel Numerical Approach for Handling Fractional Quantum Initial-Value Problems, Int. J. Fuzzy Log. Intell. Syst. 25 (2025), 416–430. https://doi.org/10.5391/ijfis.2025.25.4.416.

[15] F. Mainardi, Fractional Calculus: Theory and Applications, Mathematics 6 (2018), 145. https://doi.org/10.3390/math6090145.

[16] S. Kempfle, I. Schäfer, H. Beyer, Fractional Calculus via Functional Calculus: Theory and Applications, Nonlinear Dyn. 29 (2002), 99–127. https://doi.org/10.1023/a:1016595107471.

[17] K.B. Oldham, J. Spanier, The Fractional Calculus: Theory and Applications of Differentiation and Integration to Arbitrary Order, Academic Press, New York, 1974.

[18] D. del-Castillo-Negrete, Fractional Calculus: Basic Theory and Applications, Lecture Notes, Institute of Mathematics, UNAM, Mexico City, 2005.

[19] S.S. Ray, A. Atangana, S.C.O. Noutchie, M. Kurulay, N. Bildik, et al., Fractional Calculus and Its Applications in Applied Mathematics and Other Sciences, Math. Probl. Eng. 2014 (2014), 849395. https://doi.org/10.1155/2014/849395.

[20] J.A. Tenreiro Machado, M.F. Silva, R.S. Barbosa, I.S. Jesus, C.M. Reis, et al., Some Applications of Fractional Calculus in Engineering, Math. Probl. Eng. 2010 (2009), 639801. https://doi.org/10.1155/2010/639801.

[21] D. Kumar, D. Baleanu, Editorial: Fractional Calculus and Its Applications in Physics, Front. Phys. 7 (2019), 81. https://doi.org/10.3389/fphy.2019.00081.

[22] V. Tarasov, On History of Mathematical Economics: Application of Fractional Calculus, Mathematics 7 (2019), 509. https://doi.org/10.3390/math7060509.

[23] I. Petras, Special Issue: Fractional Calculus and Its Applications, Risk Decis. Anal. 7 (2018), 1–3. https://doi.org/10.3233/RDA-180138.

[24] B. Ross, The Development of Fractional Calculus 1695–1900, Hist. Math. 4 (1977), 75–89. https://doi.org/10.1016/0315-0860(77)90039-8.

[25] M.H. Annaby, Z.S. Mansour, q-Fractional Calculus and Equations, Springer, Berlin, 2012. https://doi.org/10.1007/978-3-642-30898-7.

[26] T.M. Atanacković, S. Pilipović, B. Stanković, D. Zorica, Fractional Calculus with Applications in Mechanics: Vibrations and Diffusion Processes, Wiley, 2014. https://doi.org/10.1002/9781118577530.

[27] C. Lubich, Discretized Fractional Calculus, SIAM J. Math. Anal. 17 (1986), 704–719. https://doi.org/10.1137/0517050.

[28] R. Gorenflo, Fractional Calculus, in: Fractals and Fractional Calculus in Continuum Mechanics, Springer, Vienna, 1997: pp. 277–290. https://doi.org/10.1007/978-3-7091-2664-6_6.

[29] M. Chen, W. Deng, Discretized Fractional Substantial Calculus, ESAIM: Math. Model. Numer. Anal. 49 (2015), 373–394. https://doi.org/10.1051/m2an/2014037.

[30] S. Pooseh, R. Almeida, D.F. Torres, Discrete Direct Methods in the Fractional Calculus of Variations, Comput. Math. Appl. 66 (2013), 668–676. https://doi.org/10.1016/j.camwa.2013.01.045.

[31] T. Abdeljawad, On Riemann and Caputo Fractional Differences, Comput. Math. Appl. 62 (2011), 1602–1611. https://doi.org/10.1016/j.camwa.2011.03.036.

[32] X. Li, K. Wu, X. Liu, Mittag–Leffler Stabilization for Short Memory Fractional Reaction-Diffusion Systems via Intermittent Boundary Control, Appl. Math. Comput. 449 (2023), 127959. https://doi.org/10.1016/j.amc.2023.127959.

[33] I. Bendib, A. Ouannas, M. Dalah, Mittag–Leffler Synchronization of Fractional-order Reaction–Diffusion Systems, Asian J. Control. (2025). https://doi.org/10.1002/asjc.3702.

[34] Y. Cao, Y. Kao, J.H. Park, H. Bao, Global Mittag–Leffler Stability of the Delayed Fractional-Coupled Reaction-Diffusion System on Networks Without Strong Connectedness, IEEE Trans. Neural Netw. Learn. Syst. 33 (2022), 6473–6483. https://doi.org/10.1109/tnnls.2021.3080830.

[35] G. Stamov, I. Stamova, C. Spirova, Reaction-Diffusion Impulsive Fractional–Order Bidirectional Neural Networks with Distributed Delays: Mittag–Leffler Stability Along Manifolds, AIP Conf. Proc. 2172 (2019), 050002. https://doi.org/10.1063/1.5133521.

[36] R.A. Askey, R. Roy, Gamma Function, in: NIST Handbook of Mathematical Functions, Cambridge University Press, pp. 135–148, 2010.

[37] C. Goodrich, A.C. Peterson, Discrete Fractional Calculus, Springer, Cham, 2015. https://doi.org/10.1007/978-3-319-25562-0.

[38] D. Luo, Z. Luo, Uniqueness and Novel Finite-Time Stability of Solutions for a Class of Nonlinear Fractional Delay Difference Systems, Discret. Dyn. Nat. Soc. 2018 (2018), 8476285. https://doi.org/10.1155/2018/8476285.

[39] Y. Wei, Y. Chen, Y. Wei, X. Zhao, Lyapunov Stability Analysis for Nonlinear Nabla Tempered Fractional Order Systems, Asian J. Control. 25 (2022), 3057–3066. https://doi.org/10.1002/asjc.3003.